Muscarinic Receptor Activation Enables Persistent Firing in Pyramidal Neurons From Superficial Layers of Dorsal Perirhinal Cortex

Vicky L. Navaroli,[1] Yanjun Zhao,[1] Pawel Boguszewski,[1] and Thomas H. Brown[1,2]*

ABSTRACT: Persistent-firing neurons in the entorhinal cortex (EC) and the lateral nucleus of the amygdala (LA) continue to discharge long after the termination of the original, spike-initiating current. An emerging theory proposes that endogenous persistent firing helps support a transient memory system. This study demonstrated that persistent-firing neurons are also prevalent in rat perirhinal cortex (PR), which lies immediately adjacent to and is reciprocally connected with EC and LA. Several characteristics of persistent-firing neurons in PR were similar to those previously reported in LA and EC. Persistent firing in PR was enabled by the application of carbachol, a nonselective cholinergic agonist, and it was induced by injecting a suprathreshold current or by stimulating suprathreshold excitatory synaptic inputs to the neuron. Once induced, persistent firing lasted for seconds to minutes. Persistent firing could always be terminated by a sufficiently large and prolonged hyperpolarizing current; it was prevented by antagonists of muscarinic cholinergic receptors (mAChRs); and it was blocked by flufenamic acid. The latter has been suggested to inhibit a Ca^{2+}-activated nonspecific cation conductance (G_{CAN}) that normally furnishes the sustained depolarization during persistent firing. In many PR neurons, the discharge rate during persistent firing was a graded function of depolarizing and/or hyperpolarizing inputs. Persistent firing was not prevented by blocking fast excitatory and inhibitory synaptic transmission, demonstrating that it can be generated endogenously. We suggest that persistent-firing neurons in PR, EC, LA, and certain other brain regions may cooperate in support of a transient-memory system. © **2011 Wiley-Liss, Inc.**

KEY WORDS: acetylcholine; transient memory; working memory; trace fear conditioning; TRPC channels; lateral amygdala; entorhinal cortex; postsubiculum; anterior cingulate cortex

INTRODUCTION

Transient memory is essential for behavior and cognition (Baddeley, 2007; Jonides et al., 2008; Baddeley, et al., 2009). Diverse theories exist regarding the neurophysiological basis of transient memory (Durstewitz et al., 2000; Major and Tank, 2004; Teramae and Fukai, 2005; Fransen et al., 2006; Mongillo et al., 2008). Most theories can be broadly divided into two types, which are not mutually exclusive. The first focuses on enduring spiking within recurrent networks of neurons (Compte et al., 2000; Rodriguez and Levy, 2001; Constantinidis and Wang, 2004; Lau and Bi, 2005). The second type, discussed below, emphasizes nonsynaptic mechanisms that are intrinsic to individual neurons. Of immediate interest, in this respect, is the phenomenon of endogenous persistent firing, as first described in brain slices of the entorhinal cortex (EC; Egorov et al., 2002; Fransen et al., 2006; Tahvildari et al., 2007) and the lateral nucleus of the amygdala (LA; Egorov et al., 2006).

Persistent-firing neurons in EC and LA discharge for seconds to minutes after terminating a suprathreshold, current step (Egorov et al., 2002; Fransen et al., 2006; Reboreda et al., 2007; Tahvildari et al., 2007). The capacity for persistent firing in these neurons is enabled by activating muscarinic cholinergic receptors (mAChRs). A rapidly-emerging theory proposes that mAChR-enabled persistent firing supports the transient memory function that is required to associate stimuli that are separated in time (Egorov et al., 2002; McGaughy et al., 2005; Fransen et al., 2006; Hasselmo, 2006; Hasselmo and Stern, 2006; Kholodar-Smith et al., 2008b; Bang and Brown, 2009; Esclassan et al., 2009; Reboreda et al., 2011). Several lines of evidence indicate that mAChR activation is critical for aspects of working or transient memory (Seeger et al., 2004; McGaughy et al., 2005; Hasselmo and Stern, 2006; Bang and Brown, 2009; Esclassan et al., 2009; Yoshida and Hasselmo, 2009).

This study asked whether neurons in perirhinal cortex (PR) also exhibit mAChR-enabled persistent firing. PR is immediately adjacent to LA and EC and is reciprocally connected to both structures (Burwell and Amaral, 1998a,b; Pitkanen et al., 2000; Pikkarainen and Pitkanen, 2001; Furtak et al., 2007b; Kerr et al., 2007). Persistent-firing neurons in both PR and EC have been hypothesized to support trace fear conditioning (Kholodar-Smith et al., 2008b; Bang and Brown, 2009; Esclassan et al., 2009), a Pavlovian paradigm in which a temporal gap (a "trace" interval) separates the offset of the conditional stimulus (CS) from the onset of the unconditional stimulus (US). The trace interval commonly lasts 10–30 s (McEchron et al., 1998; Bangasser et al., 2006; Moyer and Brown, 2006). Trace fear conditioning is severely impaired by damage to PR (Kholodar-Smith et al., 2008b) and by infusing PR with a nonselective mAChR antagonist (scopolamine; Bang and Brown,

[1] **Department of Psychology, Yale University, New Haven, Connecticut;**
[2] **Department of Cellular and Molecular Physiology, Yale University, New Haven, Connecticut**
Grant sponsor: NIA; Grant number: AG19645; Grant sponsor: NIH; Grant number: MH58405;
*Correspondence to: Thomas H. Brown, Department of Psychology, Yale University, 2 Hillhouse Ave., New Haven, CT 06520.
E-mail: thomas.brown@yale.edu
Accepted for publication 21 July 2011
DOI 10.1002/hipo.20975
Published online in Wiley Online Library (wileyonlinelibrary.com).

2009). PR infusion with scopolamine had no effect on delay fear conditioning or context conditioning, procedures in which the CS and US are not separated by a trace interval. This study demonstrated that mAChR-enabled persistent-firing is prevalent among pyramidal neurons from layer II/III of rat PR.

METHODS

Procedures involving animal subjects have been reviewed and approved by Institutional Animal Care and Use Committee of Yale University, conform to NIH guidelines, and were carried out with strict adherence to all university regulations. The methods were chosen to enable direct comparisons with hundreds of previous whole-cell recordings (WCRs) from rat PR neurons (Faulkner and Brown, 1999; Beggs et al., 2000; McGann et al., 2001; Moyer et al., 2002; Moyer and Brown, 2007). In these previous recordings, which were from rat PR brain slices bathed in artificial cerebral spinal fluid (aCSF), none of the cells exhibited persistent firing in response to either direct depolarization or excitatory synaptic stimulation. Based on this fact, we reasoned that even a small increase in the probability of persistent firing should be detectable in a sample of about 100 neurons.

Brain Slice Preparation

The preparation and imaging of PR brain slices, along with the neurophysiological methods, have been described elsewhere in considerable detail (Moyer and Brown, 2007). Briefly, male Sprague-Dawley rats (13–31 days) were deeply anesthetized with halothane and decapitated. The brain was quickly removed and placed in ice-cold oxygenated (95% O_2/5% CO_2) sucrose-aCSF containing (in mM): 206 sucrose, 2.8 KCl, 1 $CaCl_2$, 1 $MgCl_2$, 2 $MgSO_4$, 1.25 NaH_2PO_4, 26 $NaHCO_3$, and 10 D-glucose for about 3 min. The brain was blocked and glued to the tray of a temperature-controlled vibratome (Vibratome 3000, Vibratome Company, MO). Coronal slices (300 μm) containing PR were cut at ~1°C.

Slices were immediately moved to a 24-well slice incubation chamber (see Moyer and Brown, 2007), which was maintained at room temperature (22–28°C). The oxygenated aCSF (pH 7.4; 295 mOsmol) contained (in mM): 124 NaCl, 2.8 KCl, 2 $CaCl_2$, 2 $MgSO_4$, 1.25 NaH_2PO_4, 26 $NaHCO_3$, and 10 D-glucose. After at least 1 hr in the incubation chamber, individual slices were transferred to a submerged-type recording chamber, where they continued to be perfused with oxygenated aCSF. Recordings were performed on slices maintained at 31°C using an automatic temperature controller (Warner Instrument Co, Hamden, CT).

Electrical Stimulation and Recording

The WCR pipettes (3–5 MΩ) were fabricated from thin-walled glass capillaries (i.d., 1.12 mm, o.d. 1.5 mm; WPI) using a Sutter Instruments model P-97 puller. The standard pipette solution (pH 7.3; 290 mOsmol) contained (in mM): 110 K-gluconate, 10 HEPES, 20 KCl, 2.0 $MgCl_2$, 2.0 Na_2ATP, 0.3 Na_3GTP, and 10 phosphocreatine (di-Tris). The electrode resistance was calculated from the current that was required to produce a 5 mV hyperpolarizing voltage step. The seal resistance was calculated from the current that was required to produce a 20 mV hyperpolarizing voltage step. Recordings used an Axopatch 200B amplifier (Axon Instruments, CA) in current-clamp mode. Methods for capacitance and series-resistance compensation are described elsewhere (Moyer and Brown, 2007). Signals were filtered at 2 kHz, digitized at 44 kHz online using an Instrutech ITC-16 (Great Neck, NY), and acquired in real time with custom data acquisition and analysis software written using IgorPro (ver. 5.0; Wavemetrics, Lake Oswego, OR). Current steps were controlled by a Master-8 pulse stimulator (A.M.P.I., Israel) or by a programmable digital-to-analog (DAC) converter (RP2.1 Real-Time Processor, Tucker-Davis Technologies, Alachua, FL).

PR neurons were visualized using either of two upright microscopic systems. The first was a Zeiss Axioskop equipped with infrared-filtered (IR) light, differential interference contrast (DIC) optics, a Hamamatsu C2400 video camera, and a video enhancement device, as previously described (Faulkner and Brown, 1999; Beggs et al., 2000; McGann et al., 2001; Moyer et al., 2002; Moyer and Brown, 2007). The second microscope was an Olympus upright (BX51) that was similarly equipped for IR-DIC imaging. With either microscope, cells were imaged using a 60× water-immersion lens (NA 0.9).

Because of the extreme neuroanatomical and neurophysiological diversity of PR neurons (Faulkner and Brown, 1999; Beggs et al., 2000; McGann et al., 2001; Moyer et al., 2002; Furtak et al., 2007a; Moyer and Brown, 2007), recordings were restricted to upright pyramidal neurons with cell bodies in layer II/III of dorsal PR (Area 36). The rationale was that this subset of PR neurons might be most homogeneous. Pyramidal neurons constitute about half of the total number of neurons in layer II/III (Furtak et al., 2007a). Healthy pyramidal neurons were visually selected for WCRs based on IR-DIC images, as previously described (Faulkner and Brown, 1999; Moyer and Brown, 2007). To be included in the analysis, cells had to exhibit overshooting action potentials, a resting potential of −60 mV or more negative, and an input resistance of at least 120 MΩ. None of the cells included in the analysis died or became unstable during the experiment. Cells were first recorded in aCSF and then again after adding 10 μM carbachol to the aCSF. As in previous studies of persistent firing, the membrane potentials reported here were not corrected for junction potentials (about −13 mV; Moyer and Brown, 2007).

The firing patterns that were directly elicited by just suprathreshold depolarizations were classified as described elsewhere (Faulkner and Brown, 1999; Moyer and Brown, 2007; see Results). In some experiments, a bipolar concentric stimulating electrode (o.p. 200 μm SS; i.p. 50 μm Pt/Ir, FHC, Bowdoinham, ME) was placed in layer I of PR using a 4× objective. Stimulation of layer I evoked excitatory post-synaptic potentials

(EPSPs) in layer II/III pyramidal cells (Faulkner and Brown, 1999; Beggs et al., 2000; Moyer and Brown, 2007). The current was adjusted so that a single stimulation elicited a suprathreshold EPSP when the somatic membrane potential was maintained at -60 ± 1 mV. In an attempt to induce persistent firing, the input was then stimulated at 20 Hz for 2 s.

The possibility of antidromic responses was eliminated based on the subthreshold evoked waveform (the EPSP) and the suprathreshold evoked waveform (an action potential arising from the EPSP). In contrast to orthodromic responses, antidromic responses are all-or-nothing functions of the stimulus intensity and they emerge from the baseline rather than from an EPSP. We have never observed antidromic responses using the present stimulation and recording procedures, possibly because layer II/III pyramidal cell axons tend not to project to layer I.

All drugs were bath-applied at the desired concentrations. The APV (DL-2-amino-5-phosphonovaleric acid), carbachol, atropine, pirenzipine, and 4-DAMP (4-diphenyl-acetoxy-N-methyl-piperidine) stock solutions were dissolved in distilled water and then diluted to the final concentration with aCSF. The DNQX (6-cyano-7-nitroquinoxaline-2,3-dione), AFDX-116, PD102807 and flufenamic acid stock solutions were dissolved in DMSO. When stock solutions were made in DMSO, the final concentration of DMSO in the aCSF was $\leq$1%. Picrotoxin was made fresh in aCSF each time. The final drug concentrations in the bath are given in the Results section.

Persistent Firing during Noise Injections

For persistent firing to serve its hypothesized mnemonic functions, it cannot be brittle in the face of random synaptic fluctuations. Here, we illustrate the effects of three different bandwidths of Gaussian current noise at two different amplitudes. The noise amplitudes were defined by their standard deviations, which were chosen to be roughly comparable to the amplitudes of spontaneous and evoked postsynaptic currents in PR neurons (Faulkner and Brown, 1999; Beggs et al., 2000; Moyer et al., 2002; Moyer and Brown, 2007). White noise with a Gaussian amplitude distribution was generated using a programmable digital-to-analog (DAC) converter (RP2.1 Real-Time Processor, Tucker-Davis Technologies, Alachua, FL). The noise was band-pass filtered with a lower cutoff at 1 Hz and upper cutoffs at 20, 50, or 500 Hz. Finally, the standard deviation of the current noise was adjusted to be 0, 20, or 50 pA (Fig. 5). The current noise was subthreshold for directly eliciting firing. Noise was introduced 60–120 s before the first current step and it continued throughout the recording window. Firing was directly elicited by a 100 pA depolarizing current that lasted 2 s.

Statistical Analysis

The statistical significance of differences in-group means was determined using *t* tests or *F* tests. Differences in relative frequencies were evaluated using χ^2 tests. Correlations between continuous and true dichotomous variables were computed using a point-biserial correlation (r_{pb}). The standard error is denoted SE.

RESULTS

Neurophysiology of Persistent Firing

Adjustment of the resting potential

In the first group of experiments, WCRs were made from 99 cells in PR brain slices that were initially bathed in aCSF and then in aCSF containing 10 μM carbachol. Before the carbachol infusion, the mean (±SE) resting potential was -68.0 ± 0.5 mV and the mean input resistance was 183.7 ± 5.7 MΩ. After infusing carbachol, the mean resting potential was -63.3 ± 0.5 mV and the mean input resistance was 219.5 ± 7.5 MΩ. The carbachol-produced depolarization ($t_{(98)} = 10.9$; $P < 0.001$) was expected from previous studies (Egorov et al., 2002; Fransen et al., 2006). The 4.7 mV depolarization never caused spontaneous firing. In an effort to create greater neurophysiological uniformity, a steady depolarizing or hyperpolarizing current was injected into each cell to adjust the resting membrane potential to -60 ± 1 mV, which was the minimum resting potential for initial inclusion in the study (see Methods). After adding carbachol, the adjustment required a depolarizing current in 66 cells, a hyperpolarizing current in 25 cells, and no current in 8 cells. Little current was required because of the large input resistance of these cells (>120 MΩ; see Beggs et al., 2000). The carbachol-induced depolarization was clearly not the cause of persistent firing, since the same depolarization in the absence of carbachol failed to enable persistent firing.

Prevalence, rate, duration, and termination of persistent firing

In agreement with hundreds of previous recordings from PR neurons (Faulkner and Brown, 1999; Beggs et al., 2000; McGann et al., 2001; Moyer et al., 2002; Moyer and Brown, 2007), persistent firing could not be elicited while the slices were being bathed in aCSF. However, after infusion with aCSF plus 10 μM carbachol, depolarizing current steps induced persistent firing lasting at least 10 s in 85% of the cells (84/99). Figures 1–7 show representative examples of persistent firing in various experimental conditions or protocols. As discussed below, different rates of persistent firing were sometimes intentionally induced in the same neuron (see Figs. 2–4). Among the 84 cells that exhibited at least 10 s of persistent firing, the mean (± SE) lower rate of persistent firing was 1.84 ± 0.9 Hz. The mean upper rate of persistent firing was 2.56 ± 0.12 Hz.

The mean duration of persistent firing was not determined because repetitive firing was usually terminated by the experimenter (84/99 cells), based on practical considerations. Bearing this in mind, the observed duration distribution was as follows:

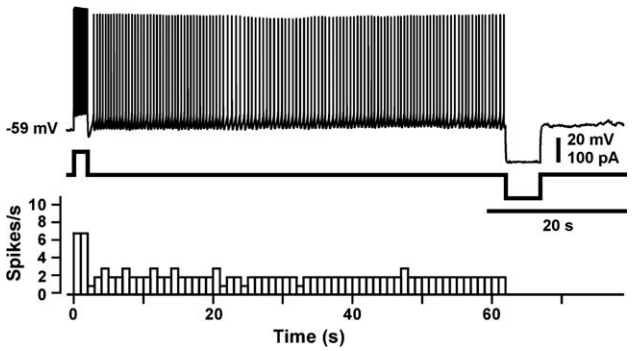

FIGURE 1. Induction and termination of persistent firing. Top: the upper and lower items are voltage responses and current steps, respectively. The depolarizing current step was suprathreshold for directly eliciting repetitive firing and for inducing persistent firing. Persistent firing was terminated after a minute by a hyperpolarizing current step. Bottom: the histogram shows the number of spikes in successive 1-s time bins during and after the current step. In this figure and all others, the displayed record of persistent firing includes all of the digitally recorded data.

1–9 s (n = 9), 10–19 s (n = 3), 20–29 s (n = 34), 30–39 s (n = 35), 40–49 s (n = 7), 50–59 s (n = 0), 60–69 s (n = 3), 70 s or longer (n = 2). Persistent firing failed to occur in 7% (6/99) of the cells. In these six neurons, a depolarizing after-potential (DAP) was evident following the offset of the current step. Examples of DAPs are illustrated in Figures 3 and 6. At some point in each recording, persistent firing was completely terminated by a large and prolonged hyperpolarization (see Fig. 1). Following its termination, persistent firing could always be reinduced by a second depolarization.

In a subset of these cells (57/99 neurons), the experimental protocol included recordings lasting at least 30 s after the offset of the depolarizing stimulus. Eighty-three percent of these neurons (47/57 neurons) exhibited persistent firing lasting at least 30 s. Since there are known developmental changes in persistent firing in EC (Reboreda et al., 2007), we examined the relationship between the age of the animals, which ranged from 13 to 30 days old, and the occurrence of persistent firing. The mean ($\pm$ SE) age was 21 $\pm$ 1 days. There was no significant correlation between the age of the animals and the occurrence of 30 s of persistent firing ($r_{pb(57)} = -0.16$; $P = 0.90$). In this group of 57 neurons, no attempt was made to induce different rates of persistent firing. The mean firing rate was 1.86 $\pm$ 0.12 Hz (n = 47). Twelve percent of the cells exhibited persistent firing that lasted <10 s (7/57 neurons). Five percent of the cells (3/57 neurons) failed to exhibit persistent firing. In these three cells, a DAP was evident after the offset of the current step.

Figure 1 shows an example of persistent firing that was allowed to continue for 60 s. The frequency-time histogram gives the number of action potentials in successive 1-s intervals. After a minute of continuous discharge, persistent firing was terminated by a hyperpolarizing current step. The longest duration of persistent firing was terminated after 3 min. Additional examples of persistent firing, lasting 30 s or longer, are illustrated in Figures 4, 5, and 7.

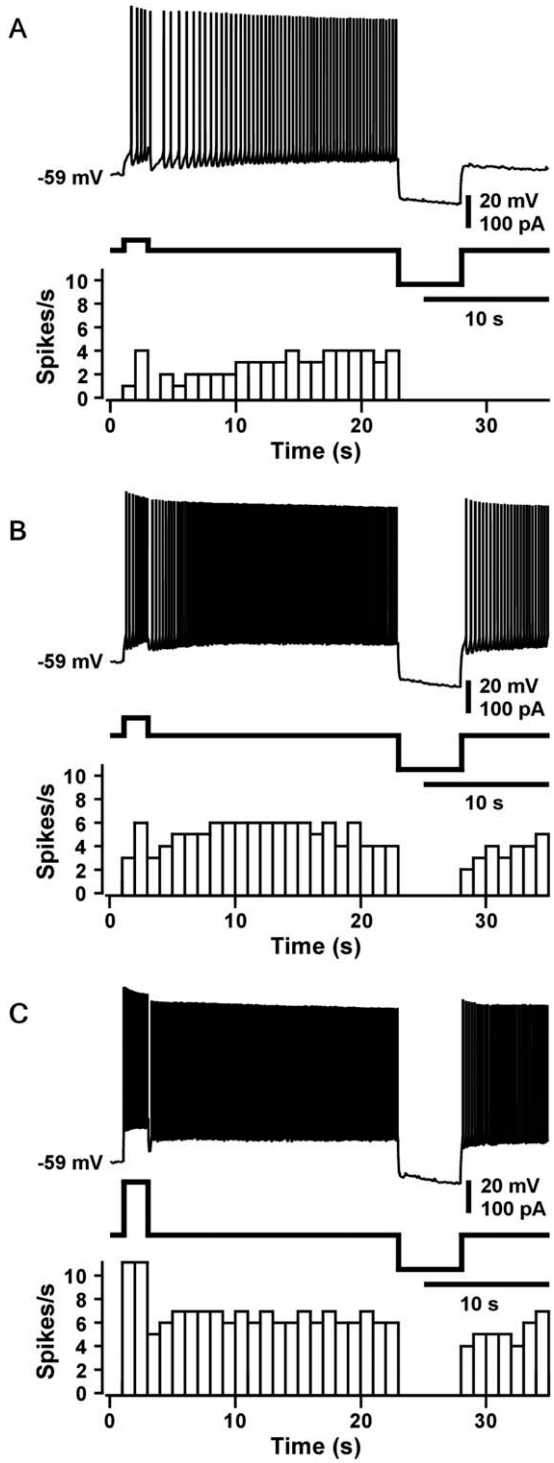

FIGURE 2. Graded nature of persistent firing. The left-hand side of the traces shows persistent firing rates produced in the same neuron by current steps with three different amplitudes (A–C). Depending on the rate of persistent firing, a subsequent hyperpolarizing current step either terminated firing (A) or reduced the rate of persistent firing (B and C). In every case, firing terminated during the hyperpolarization. The histogram shows the number of spikes in successive 1 s time bins.

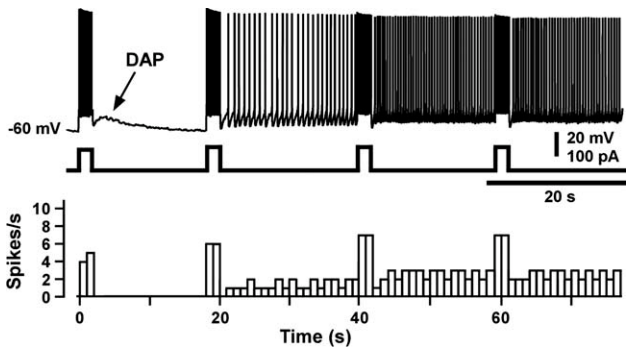

FIGURE 3. Graded-persistent firing and temporal integration. The amplitude of the first 2 s current step was adjusted to be suprathreshold for firing the cell, but subthreshold for evoking persistent firing. Note that it generated a depolarizing after potential (DAP). The second application of the same current step induced persistent firing. The third current step increased the rate of persistent firing, while the fourth step produced no further effect. The time histogram shows the number of spikes in successive 1 s time bins.

Firing patterns during the depolarizing current step

In direct response to a depolarizing current step, different PR neurons can exhibit one of six distinguishable firing patterns (Faulkner and Brown, 1999; Moyer and Brown, 2007). The frequency distribution of firing patterns varies as a joint function of the morphological cell type and the cortical layer. All of the cells recorded in the present study exhibited either a regular-spiking (RS) or a late-spiking (LS) firing pattern, as expected based on previous studies of layer II/III pyramidal neurons (Faulkner and Brown, 1999; Beggs et al., 2000; Moyer and Brown, 2007). Thirty-eight cells were classified as RS neurons. Of these, 29 showed persistent firing (76%). Sixty-one cells were classified as LS neurons, 55 of which showed persistent firing (90%). There was no significant relationship between the firing pattern elicited by the current step and the occurrence of persistent firing ($\chi^2_{(1)} = 2.0$; $P = 0.16$). These results do not necessarily generalize to other cell morphologies or firing patterns in PR. In addition to the RS and LS neurons recorded in this study, other firing patterns include fast-spiking, burst-spiking, single-spiking, and irregular spiking (Faulkner and Brown, 1999; Moyer and Brown, 2007).

Graded nature of persistent firing

The graded or analog nature of persistent firing was explored using three methods that were borrowed from studies of persistent firing in EC (Egorov et al., 2002; Fransen et al., 2006; Tahvildari et al., 2007) and LA (Egorov et al., 2006). The first approach asked whether the rate of persistent firing depends on the amplitude of the spike-eliciting current step. This procedure was applied to 9 of the 47 cells in which recordings lasted at least 30 s after the offset of the current step. An example of the effect of the current amplitude on the rate of persistent firing is illustrated on the left-hand side of Figure 2 (before the hyperpolarizing current step). The histograms show the numbers of spikes in successive 1-s time bins.

As expected, increasing the current-step amplitude increased the firing rate during the current step. The mean firing rates ($n = 9$) during the smallest, intermediate, and largest current steps, respectively, were 2.95 ± 0.22, 5.35 ± 0.18, and 6.40 ± 0.13 Hz ($F_{(2, 38)} = 130.4$; $P < 0.001$). When tested on a single-cell basis, the effect of the current-step amplitude on the persistent-firing rate was statistically significant (F tests; $P < 0.05$) in seven of the nine cells that were tested. In the remaining two cells, the smallest tested current that caused persistent firing resulted in almost the maximum rate of persistent firing.

The second method examined the effect of a 5 s hyperpolarizing current step on the rate of persistent firing ($n = 25$). In every case, firing ceased during the current step. In all 25 cells, the hyperpolarization either terminated persistent firing or reduced the rate of persistent firing. As shown in the right-hand part of Figure 2, the effect of a hyperpolarizing current step of fixed amplitude (110 pA) depended on the persistent-firing rate prior to the hyperpolarization. When the persistent-firing rate was lowest (Fig. 2A), the hyperpolarizing current step terminated firing. When the persistent-firing rate was somewhat higher, the same hyperpolarizing current step, applied to the same cell, failed to terminate firing, but it did reduce the mean rate of persistent firing (Fig. 2B).

In the example illustrated in Figure 2B, the mean rate of persistent firing in response to an intermediate current step was 5.35 ± 0.18 Hz before the hyperpolarization and 3.57 ± 0.37

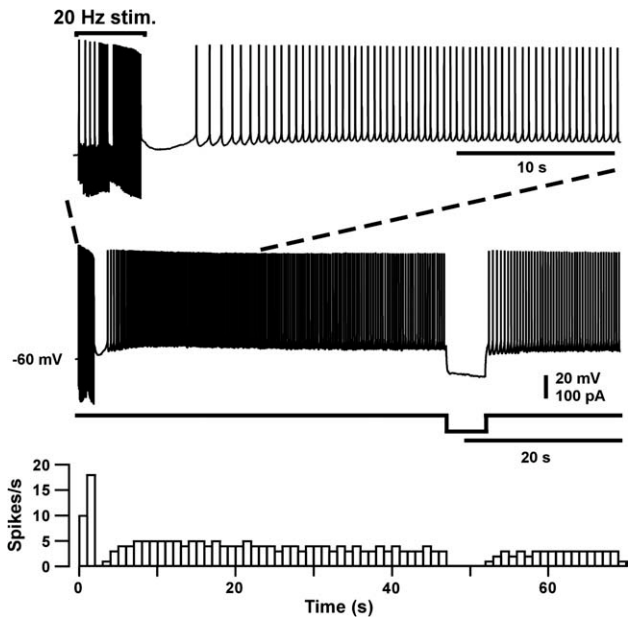

FIGURE 4. Persistent firing induced by synaptic stimulation. The top trace shows the onset of persistent firing and the bottom trace illustrates the first 70 s, during which data were stored. The histogram gives the number of spikes in successive 1 s time bins. Persistent firing was completely blocked during the prolonged hyperpolarizing current injection. Repetitive firing resumed after the offset of the hyperpolarizing current step, but a lower rate than before the hyperpolarization.

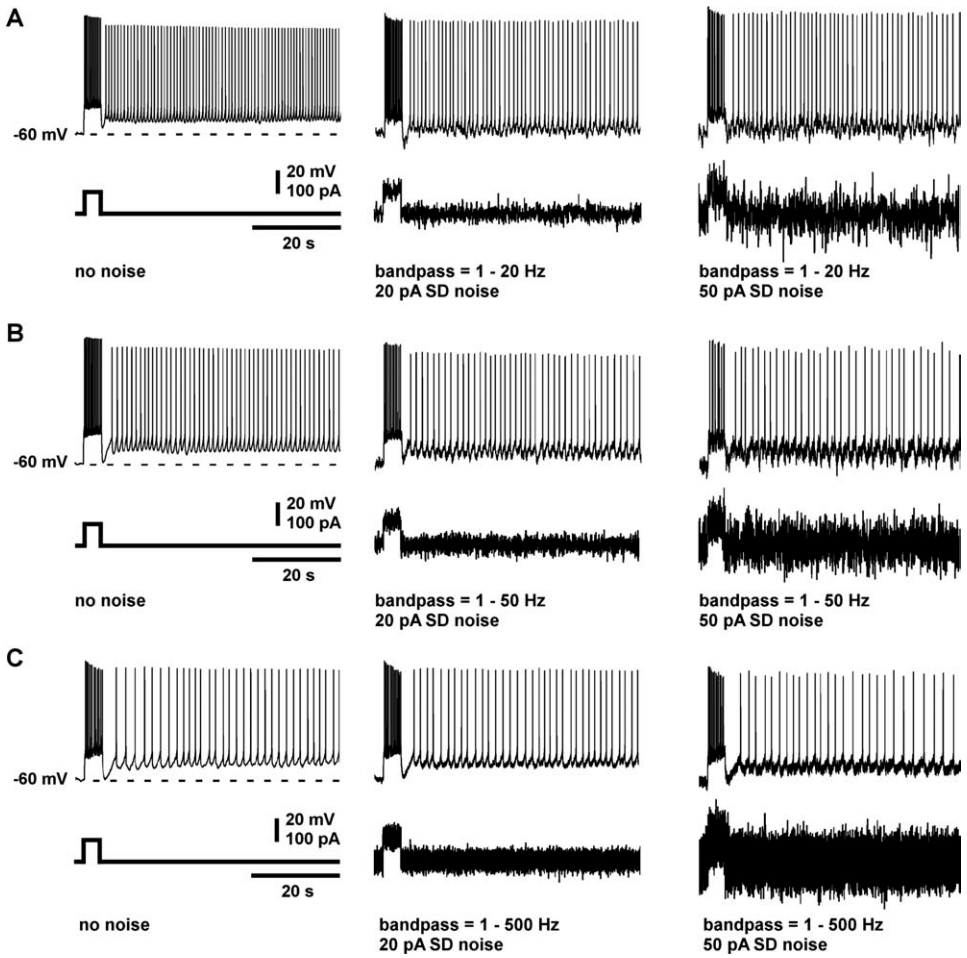

FIGURE 5. Persistent firing in the presence of noise. The amplitude of the added noise, measured by its standard deviation (SD), was 0 pA (left column), 20 pA (middle column), or 50 pA (right column). Noise was filtered at 1–20 Hz (A), 1–50 kHz (B), or 1–500 Hz (C). None of the noise conditions blocked persistent firing.

Hz after the hyperpolarization. This 33% reduction in the firing rate was statistically significant ($t_{(6)} = 6.97$; $P < 0.001$), based on firing rates in the 7 time bins (1 s each) before and after the hyperpolarization. In the same cell, illustrated in Figure 2C, the mean firing rate during a larger current step was 6.40 ± 0.13 Hz before the hyperpolarization and 5.14 ± 0.40 Hz after the hyperpolarization. This 20% reduction was also statistically significant based on the same time bins ($t_{(6)} = 2.714$; $P < 0.05$). When tested on a single-neuron basis, these reductions in firing rate were statistically significant in 22 of the 25 cells (t tests; $P < 0.05$). In the remaining three neurons, the hyperpolarization was also accompanied by a reduction in the firing rate, but the firing-rate change was not statistically significant. In the example shown in Figure 2, the reductions in the persistent-firing rates may not have been long lasting. Following the reinstatement of firing, the discharge rates were gradually increasing during the recorded interval. Figure 4, discussed below, illustrates a longer-duration reduction in the firing rate. As noted earlier, persistent firing could always be terminated by a sufficiently large and prolonged hyperpolarization.

The third procedure was to inject one or more depolarizing currents after the onset of persistent firing ($n = 13$). An example is shown in Figure 3, where the frequency-time histogram gives the number of action potentials in successive 1-s time bins. The first current step was suprathreshold for eliciting a train of action potentials (at 4–5 spikes per 1-s time bin) and a DAP, but it was subthreshold for inducing persistent firing. The second current step directly elicited firing at six spikes per time bin, and it induced persistent firing at one or two spikes per time bin. The qualitative difference between the effect of the first and second current steps suggests that some residuum of the first depolarization must have persisted during the 16 s interval between the offset of the first current step and the onset of the second. Note that repetitive depolarizations were not necessary to trigger persistent firing. A sufficiently large initial depolarization always elicited persistent firing in cells that are capable of this discharge pattern.

The mean persistent-firing rates after the second and third current steps were significantly different from each other ($t_{(16)} = 7.78$; $P < 0.001$), based on a comparison of the 17 time bins before and after the second current step. There was no

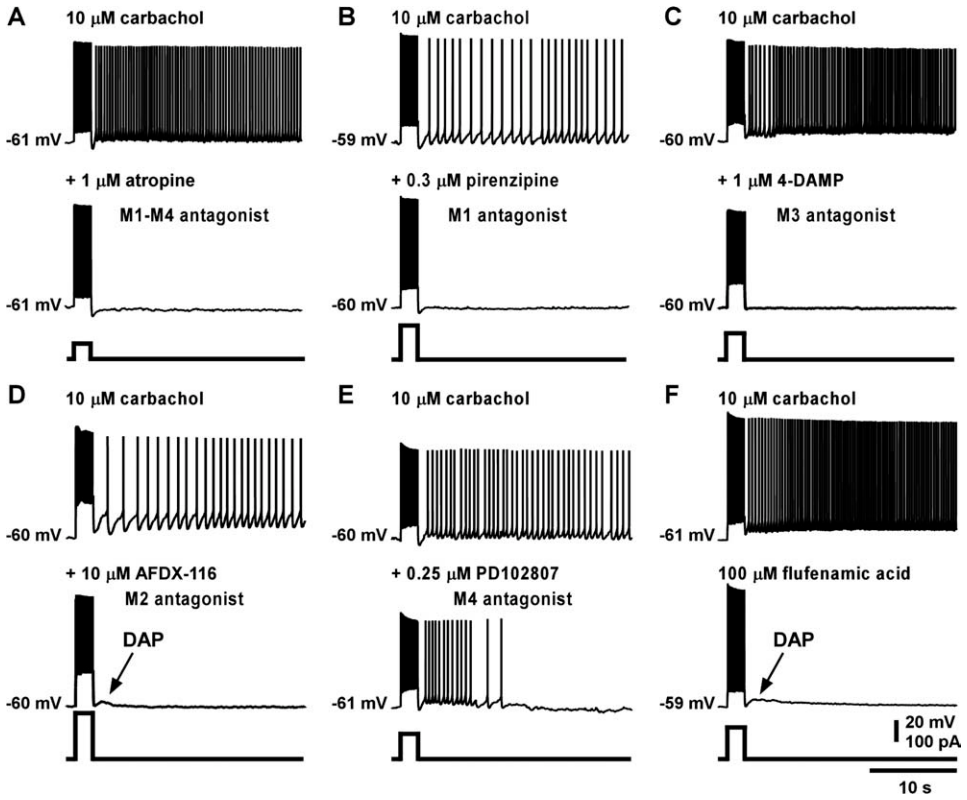

FIGURE 6. Neuropharmacology of persistent firing. (A) Atropine (1 μM), a general mAChR antagonist, blocked the DAP and persistent firing. (B and C) Pirenzipine (0.3 μM), an M1 receptor antagonist, and 4-DAMP (1 μM), an M3 receptor antagonist, also blocked the DAP and persistent firing. In the illustrated cells and in all others, M1 and M3 receptor antagonists acted like atropine. (D) AFDX-116 (10 μM), an M2 receptor antagonist, blocked persistent firing, but a DAP remained. (E) PD102807 (0.25 μM), an M4 receptor antagonist, allowed brief persistent firing in the illustrated cell but not in others. (F) Flufenamic acid (100 μM) blocked persistent firing, leaving a DAP.

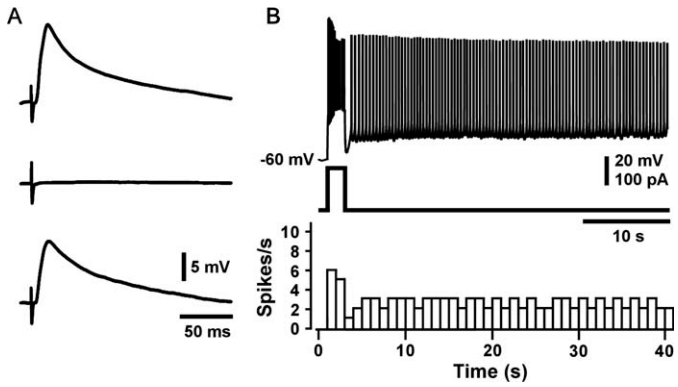

FIGURE 7. Endogenous persistent firing. (A) Fast synaptic transmission was reversibly blocked by two glutamatergic receptor antagonists (50 μM APV and 10 μM DNQX) and a GABAergic receptor antagonist (100 μM picrotoxin). The illustrated traces are averages of five successive evoked excitatory postsynaptic potentials (EPSPs). The top trace is the evoked PSP before applying the receptor antagonists. The middle trace shows the complete EPSP block during the drug application. The bottom trace shows the EPSP recovery after the antagonists were washed from the bath. (B) Persistent firing elicited by a depolarizing current step during the period in which the EPSP was blocked.

significant difference between the mean firing rates following the third and fourth current steps, which directly elicited firing at 7 spikes per 1-s bin, followed by persistent firing at 2–3 spikes per bin. Further statistical analysis compared the effects of the two smallest current steps that elicited persistent firing. Eight of the 13 cells showed a statistically significant increase in firing rate (t tests, $P < 0.05$) following the larger of the two current steps. In the group as a whole, the mean persistent-firing rate following the smallest depolarization that elicited persistent firing (2.18 ± 0.25 Hz) was significantly lower than the mean firing rate following the next-largest depolarization (2.54 ± 0.26 Hz; $t_{(12)} = 2.99$; $P < 0.05$).

In summary, graded persistent firing is common among pyramidal neurons from superficial layers of dorsal PR. The graded nature of persistent firing eliminates a whole class of candidate mechanisms that would result in strictly bi-stable states (Brody et al., 2003; Fransen et al., 2006).

Persistent firing elicited by synaptic stimulation

Persistent firing was readily elicited by stimulating excitatory synaptic inputs to the recorded neuron (4/4 cells tested). As in

the previous experiments, the slices were bathed in aCSF containing 10 μM carbachol. A typical example is illustrated in Figure 4, where the time histogram again gives the number of action potentials in successive 1-s time bins. During the synaptic stimulation, the firing rate ranged from 10 to 17 spikes/bin. The subsequent rate of persistent firing peaked at 5 spikes/bin and then gradually declined to 3–4 spikes/bin. Following a hyperpolarizing current step, the rate stabilized at 3 spikes/bin. This decrease in the firing rate was statistically significant ($t_{(17)} = 9.22$; $P < 0.001$), based on the 18 time bins (1 s each) before and after the current step.

Among the four neurons that were tested, the rate of synaptically elicited persistent firing ranged from 1.6 to 4.1 Hz. The mean (± SE) firing rate was 2.61 ± 0.26 Hz. After terminating persistent firing, with a sufficiently large and prolonged hyperpolarizing current step, it could be re-elicited by a second synaptic stimulation and/or by a second depolarizing current step (4/4 cells). Repetitive suprathreshold synaptic stimulation does not cause persistent firing in layer II/III pyramidal neurons bathed in aCSF (Beggs et al., 2000; also see Moyer and Brown, 2007).

Persistent firing during random current noise

The hypothesis that persistent firing mediates aspects of transient memory requires that the underlying mechanism be robust to random noise and distracters (Brody et al., 2003; Fransen et al., 2006). An additional set of experiments ($n = 8$ cells) examined persistent firing in the presence of Gaussian current noise of three different amplitudes and in three different frequency bands (see Methods). Representative results are illustrated in Figure 5. The three rows (A–C) are recordings from three different neurons that were subjected to noise in three different frequency bands: 1–20 Hz (top row); 1–50 Hz (middle row), and 1–500 Hz (bottom row). The three columns illustrate the effects of increasing the amount of current noise, measured by its standard deviation (SD), which was either 0 pA (left column, no-noise control condition), 20 pA (middle column), or 50 pA (right column). Persistent firing was not blocked in any of the noise conditions (8/8 cells).

Neuropharmacology of persistent firing

Antagonists of muscarinic cholinergic receptors. Several mAChR antagonists demonstrated that the pharmacological action of carbachol on persistent firing was mediated by mAChRs. Atropine (1 μM), an antagonist of all mAChR-receptor subtypes, blocked both persistent firing and DAPs ($n = 5$; Fig. 6A). More selective antagonists of M1–M4 receptors were also explored. Pirenzipine (0.3 μM; $n = 3$; Fig. 6B), an M1 receptor antagonist, blocked persistent firing (3/3 neurons), as did 4-DAMP (1 μM; $n = 5$; Fig. 6C), an M3 receptor antagonist (5/5 neurons). Both antagonists also blocked DAPs.

Perfusion with the M2 and M4 receptor antagonists, AFDX-116 and PD102807, respectively, produced more variable effects on persistent firing and DAPs. Following infusion with AFDX-116 (10 μM; $n = 7$), none of the tested cells showed persistent firing, but DAPs remained in three of the seven neurons (see Fig. 6D). Following the infusion with PD102807 (0.25 μM; $n = 5$), only one of the four tested cells continued to show persistent firing. In this cell, the firing rate was low and it self-terminated several seconds after the offset of the current step (Fig. 6E). A DAP remained in three cells that did not exhibit persistent firing. Thus, at the tested concentrations, antagonists for M1 and M3 receptors were comparable to atropine in blocking persistent firing and DAPs, whereas the M2 and M4 antagonists were not comparable to atropine.

Antagonist of a nonspecific cation conductance. According the standard hypothesis (Egorov et al., 2002; Fransen et al., 2006), the sustained current supporting endogenous persistent firing in EC and LA is a Ca^{2+}–dependent, nonspecific, cation conductance (G_{CAN}) that is activated by the combination of agonist binding to mAChRs and a large elevation in the intracellular Ca^{2+} concentration ($[Ca^{2+}]_i$). Flufenamic acid reliably blocks persistent firing in LA and EC, presumably by inhibiting G_{CAN} (Egorov et al., 2002; Fransen et al., 2006). Perfusion with flufenamic acid (100 μM) reliably eliminated persistent firing (5/5 neurons; Fig. 6F). Recently, flufenamic acid was also shown to block mAChR-enabled persistent firing in the postsubiculum (PoS; Yoshida and Hasselmo, 2009) and in the anterior cingulate cortex (ACC; Zhang and Seguela, 2010). Although the specificity of flufenamic acid for G_{CAN} can be questioned (Wang et al., 2006), the results demonstrate another parallel to findings in other brain regions.

Antagonists of ionotropic glutamate and GABA receptors. An additional 23 neurons were studied under conditions in which fast synaptic transmission through ionotropic receptors was blocked. As in the earlier-described group of 57 cells, recordings in this group of 23 neurons lasted at least 30 s after the offset of the initial depolarizing current. The ages of the animals ranged from 13 to 31 days old. The mean age (± SE) was 21 ± 1 days. The point-biserial correlation between the age of the animal and the occurrence of 30 s of persistent firing was not statistically significant ($r_{pb(21)} = 0.13$; $P = 0.55$). Thus, the ages of the animals were quite similar in both groups and in neither group was there a significant correlation between age and the occurrence of 30 s of persistent firing.

As before, persistent firing was studied in brain slices bathed in aCSF plus carbachol (10 μm). The position of the extracellular stimulating electrodes and the amount of current were adjusted to produce a reliable excitatory postsynaptic potential (EPSP; Fig. 7A). Next, fast synaptic transmission was blocked by perfusing the slices with 50 μM APV (an NMDA receptor antagonist), 10 μM DNQX (an AMPA receptor antagonist), and 100 μM picrotoxin (a $GABA_A$ receptor antagonist). The cell featured in Figure 7 demonstrates persistent firing following the block of fast synaptic transmission. The top trace in Figure 7A shows a large EPSP before the transmission block. The middle trace demonstrates that the drug combination completely blocked the EPSP. Figure 7B illustrates persistent firing

in this same cell during the block of fast synaptic transmission. The bottom trace in Figure 7A shows the restoration of the EPSP after the neurotransmitter antagonists were washed from the bath.

During the blockade of fast synaptic transmission, 43% of the cells (10/23) exhibited persistent firing that lasted at least 30 s. In these 10 neurons, persistent firing was clearly endogenously generated. In absolute terms, the proportion of cells showing 30 s of persistent firing in this group of 23 cells was smaller than in the previously described sample of 57 cells. However, the difference in proportions did not approach statistical significance ($\chi^2_{(1)} = 2.0$; $P = .157$). As in the first set of experiments, persistent firing was always completely terminated by a hyperpolarizing current step. The mean rate of persistent firing under these conditions was 2.13 ± 0.21, which is similar to the earlier-noted rate of persistent firing in the absence of synaptic blockade.

DISCUSSION

In agreement with several previous studies of the firing patterns of rat PR neurons (Faulkner and Brown, 1999; Beggs et al., 2000; McGann et al., 2001; Moyer et al., 2002; Moyer and Brown, 2007), persistent firing was never observed while the brain slices were being bathed in aCSF ($n = 99$). The dramatic new finding is that adding 10 μM carbachol to the bath qualitatively transformed most (85%) of the neurons by enabling persistent firing. Figures 1–6 give representative examples of persistent firing in these cells under various experimental conditions. In a second set of experiments, persistent firing was recorded in slices bathed in aCSF after complete blockade of fast synaptic transmission ($n = 23$). The results demonstrate that persistent firing can be generated-endogenously. Figure 7 shows a representative example of persistent firing during the complete blockade of fast synaptic transmission. All of the recordings ($n = 122$) were from RS or LS pyramidal neurons with cell bodies in layer II/III of dorsal PR. This well-defined group furnishes a convenient and relatively homogeneous source of persistent-firing PR neurons for future cellular and molecular studies.

Some open questions include whether persistent firing occurs in ventral PR (Area 35), in other layers of dorsal or ventral PR, or in any of the numerous non-pyramidal cell types (Faulkner and Brown, 1999; Furtak et al., 2007a; Moyer and Brown, 2007). One might predict that persistent firing would not occur in single-spiking neurons, since they only fire once in response to a strong and prolonged depolarization. Similarly, persistent firing might not occur in the large, burst-firing pyramidal neurons in layer V, because bursting in these cells is normally accompanied by a large hyperpolarizing after-potential (Faulkner and Brown, 1999; Moyer and Brown, 2007). The small, fast-spiking PR neurons (Faulkner and Brown, 1999; Moyer and Brown, 2007), which are probably inhibitory local-circuit neurons, also may not exhibit persistent firing, which has thus far only been reported in large neurons. Persistent firing may be limited to the larger PR neurons, which are either pyramidal neurons or spiny stellates (Faulkner and Brown, 1999; Furtak et al., 2007a; Moyer and Brown, 2007).

Comparisons with Persistent-Firing Neurons in EC and Amygdala

In six respects, persistent firing in PR was qualitatively similar to persistent firing in EC (Egorov et al., 2002; Fransen et al., 2006; Tahvildari et al., 2007) and LA (Egorov et al., 2006). First, persistent firing in PR lasted tens of seconds to minutes (Figs. 1–7). Notably, these durations include the range of trace intervals that are commonly used in studies of trace fear conditioning (McEchron et al., 1998; Moyer and Brown, 2006; Kholodar-Smith et al., 2008b; Bang and Brown, 2009; Esclassan et al., 2009). Second, persistent firing was enabled by mAChR activation. More precisely, persistent firing was enabled by carbachol, a nonspecific cholinergic agonist, and it was reliably blocked by atropine and more selective muscarinic antagonists (Fig. 6). Third, persistent firing was reliably prevented by flufenamic acid (Fig. 6). Fourth, the discharge rate during persistent firing was relatively low (Figs. 1–7). Fifth, the persistent-firing rate was often a graded function of depolarizing and hyperpolarizing inputs to the cell (Figs. 2–4). Finally, persistent firing occurred after blockade of fast synaptic transmission (Fig. 7), demonstrating that it can be endogenously generated. Five of these characteristics of persistent firing have also been reported in neurons from PoS (Yoshida and Hasselmo, 2009) and ACC (Zhang and Sequela, 2010). Still unknown is whether these neurons can exhibit graded persistent firing.

Quantitative Effects of Recording Methods on Persistent Firing Characteristics

Variations in recording methods may cause quantitative differences in persistent-firing characteristics. Persistent firing in LA and EC has usually been evaluated using sharp electrodes or perforated-patch recordings. The rationale was that the ruptured-patch technique, used in this study, might cause "rundown" resulting from the washout of diffusible intracellular messengers. Indeed, a recent comparison between perforated-patch and ruptured-patch recordings in layer V of EC did report differences (Reboreda et al., 2007). Specifically, cells recorded in ruptured-patch configuration showed a lower probability of exhibiting graded persistent firing. In addition, the retention of graded activity greatly diminished with the passage of time.

This study used ruptured patches to allow direct comparisons with hundreds of previously recorded PR neurons. In spite of possible washout effects, the results demonstrated the existence and the prevalence of persistent-firing neurons in PR. The use of sharp electrodes or perforated-patch electrodes might have resulted in a larger proportion of persistent-firing neurons in the targeted population, a higher rate or duration of persistent firing, and/or a greater range of graded-persistent firing rates.

A second methodological difference is that the recordings in other structures were done in slices maintained at a slightly higher bath temperature (Egorov et al., 2002, 2006; Tahvildari et al., 2007; Yoshida and Hasselmo, 2009), which could have resulted in a higher persistent-firing rate. Our concern was that the combination of higher temperatures and ruptured-patch WCRs would not be favorable for stable, long-term experiments.

Involvement of PR, EC, and Amygdala in Trace Fear Conditioning

Recent behavioral analyses have identified two important similarities between PR and EC function in terms of Pavlovian fear conditioning. First, lesions of both structures severely impair trace fear conditioning without affecting delay fear conditioning (Kholodar-Smith et al., 2008b; Esclassan et al., 2009). In the delay conditioning procedures, the CS and US overlapped temporally and co-terminated, thereby obviating the requirement for transient memory (see Bangasser et al., 2006). Second, injections of mAChR antagonists into both PR and EC impaired trace but not delay fear conditioning (Bang and Brown, 2009; Esclassan et al., 2009). Additionally, the PR infusion produced no detectable effect on context conditioning (Bang and Brown, 2009), in sharp contrast to the profound effect that PR damage has on context conditioning (Bucci et al., 2000; Lindquist et al., 2004; Kolodar-Smith et al., 2008a,b). The selectivity of the mAChR antagonist for trace conditioning shows that the infusion was not simply inactivating PR function.

Based on prevailing views (Maren and Quirk, 2004; Pare et al., 2004; Fanselow and Poulos, 2005; Phelps and LeDoux, 2005; Kim and Jung, 2006; Helmstetter et al., 2008; Bach et al., 2011), one might guess that the amygdala is critically involved in all forms of Pavlovian fear conditioning. Surprisingly, however, almost nothing is known about the role of the amygdala in trace fear conditioning. One recent study (Raybuck and Lattel, 2011) concluded that the insertion a trace interval between the CS and the US causes cue conditioning to become amygdala-independent. More specifically, muscimol infusion into the amygdala of C57BL mice had no effect on trace conditioning to an auditory cue. However, as expected from previous studies, the infusion severely impaired delay conditioning to the same cue as well as conditioning to the training context. The authors report a double dissociation, as muscimol infusion into the dorsal hippocampus was found to impair trace but not delay conditioning. To the best of our knowledge, the only other experiment on the role of the amygdala in trace conditioning was one that was recently completed in our laboratory. This study found that scopolamine infusion into the rat amygdala selectively impairs trace fear conditioning without affecting delay conditioning or context conditioning (Kent et al., 2011). Additional research is clearly needed to resolve the role of the amygdala in trace conditioning. The role of the hippocampus in trace conditioning is further considered below.

Persistent Firing in Other Aspects or Mechanisms of Transient Memory

The concept that persistent firing in PR supports transient stimulus representations has implications that extends well beyond trace fear conditioning. Delayed object recognition tasks, which also require transient stimulus memory, are well known to depend on PR function (Baxter and Murray, 2001; Parsana and Brown, 2010). Furthermore, extracellular recordings from rat PR have revealed single units that maintain stimulus-specific activity during the delay period of an odor-guided version of the delayed match-to-sample task (Young et al., 1997). Recently, mAChR-enabled persistent firing in PoS was proposed to support the head-direction system in the absence of key navigational stimuli (Yoshida and Hasselmo, 2009). From another theoretical perspective (Mongillo et al., 2008), persistent firing might be imagined to help maintain transient synaptic plasticity in recurrent circuits.

Hypothesized Conductance Mechanisms Underlying Persistent Firing

The original hypothesis for persistent firing in EC, LA, and PoS (Egorov et al., 2002; Fransen et al., 2006; Yoshida and Hasselmo, 2009) proposed that Ca^{2+} influx through voltage-gated Ca^{2+} channels activates two, opposing, sustained currents. The first is a depolarizing, Ca^{2+}-dependent, nonselective cation current (I_{CAN}). The second is a hyperpolarizing, Ca^{2+}-dependent K^+ current ($I_{K(Ca)}$). Accordingly, the occurrence of persistent firing depends on the timing and the absolute and relative sizes of I_{CAN} and $I_{K(Ca)}$. Theoretically, a change in the magnitude of either of these currents could enable persistent firing. The graded nature of persistent firing was previously theorized to emerge from the dynamics of Ca^{2+}-dependent biochemical mechanisms that regulate I_{CAN} channel function (Fransen et al., 2006).

Preliminary evidence suggests that I_{CAN} may be based on transient receptor potential (TRP) channels, in particular the TRPC subfamily (Yoshida et al., 2008; Blair et al., 2009; Yan et al., 2009; Reboreda et al., 2011; Zhang et al., 2011). Importantly, some TRPC channels are gated by the combination of elevated $[Ca^{2+}]_i$ and agonist binding to extracellular receptors, including mAChRs (Ramsey et al., 2006; Venkatachalam and Montell, 2007; Blair et al., 2009; Reboreda et al., 2011). Recent evidence shows that, in layer III of EC, activation of group I metabotropic glutamate receptors (mGluRs) can also enable persistent firing, an effect that has also been attributed to TRPC channels (Yoshida et al., 2008). Interestingly, mGluR-enabled persistent firing does not depend on mAChR activation. Nothing is known about the distribution of TRPC channels and mAChRs in PR. An obvious next step, for understanding the conductance mechanisms in PR neurons, will be to determine whether or how persistent firing in PR depends on Ca^{2+} entry, elevated $[Ca^{2+}]_i$, and an increase in an inward current. Alternatively, mAChR-enabled persistent firing in PR could be supported by a decrease in a Ca^{2+}-dependent K^+ current, although this has not been reported in the other brain structures reviewed here.

Memory Buffer System and Its Remote Control

The fact that PR is reciprocally and strongly connected to LA and EC raises the possibility that persistent-firing neurons in combinations of these three structures may cooperate in the support of a regional memory buffer system. The previously described neuropharmacological experiments on trace conditioning certainly support this possibility. All three of these structures also have direct and indirect reciprocal connections with the hippocampus (HC), which presumably furnishes an important part of the input to this memory buffer (Eichenbaum et al., 1994; McEchron, et al., 1998; Quinn, et al., 2002; Chowdhury et al., 2005; Bangasser et al. 2006; Yoon and Otto, 2007; Woodruff-Pak and Disterhoft, 2008). In rats, the ventral HC is especially important for trace fear conditioning (Yoon and Otto, 2007; Czerniawski et al., 2009).

The role of the hippocampus in trace conditioning depends on both the nature of the conditional response and the trace interval. Trace fear conditioning in mice has been reported to become hippocampus-independent when the trace interval is reduced to <10 s (Misane et al., 2005). This finding seems puzzling because the hippocampus is well known to be essential for trace eyeblink conditioning (Solomon et al., 1986; Moyer et al., 1990; Woodruff-Pak and Disterhoft, 2008), where the trace intervals are always of the order of tenths of a second. The reason that such short intervals have been explored is that conditioning simply does not occur with longer intervals. Whether trace fear and eyeblink conditioning engage the same temporal bridging mechanisms is unknown. Conceivably, persistent firing might not be required for bridging very short intervals, where some other mechanism might be sufficient. At the moment, there is no information as to whether PR lesions impair trace eyeblink conditioning.

Since persistent firing is enabled by mAChR activation, an obvious next question concerns the neurophysiological control of acetylcholine release. PR, EC, and LA each receive cholinergic input from neurons in the basal forebrain (Alonso and Amaral, 1995; Vaucher and Hamel, 1995; Carlsen et al., 2004; Mesulam, 2004; Winters and Bussey, 2005; Egorov et al., 2006). Nothing is known about the ultimate neurophysiological control of firing in these cholinergic neurons, which receive both cortical and subcortical inputs. This line of reasoning predicts that cholinergic neurons should become active in tasks that require transient memory. The initial trigger for ACh release could be stimulus novelty or a more complex executive function of prefrontal cortex.

General Conclusions and Implications

The widespread occurrence of mAChR-enabled persistent firing invites a major reexamination of the neurophysiological foundations of transient memory. Persistent firing is a viable, nonsynaptic, mechanism for supporting aspects of transient memory. Notably, persistent firing is just one of several types of activity-dependent, nonsynaptic modifications that have been proposed to maintain short-term changes in cellular and circuit function (Magee and Johnston, 2005; Bucher et al., 2006; Johnston and Narayanan, 2008; Mozzachiodi and Byrne, 2010). Rapidly accumulating evidence suggests that non-synaptic modifications may play a much larger role in transient memory than previously imagined.

Acknowledgments

The authors thank Ashwini J. Parsana for assistance with the analysis and for useful comments on the manuscript.

REFERENCES

Alonso JR, Amaral DG. 1995. Cholinergic innervation of the primate hippocampal formation. I. Distribution of choline acetyltransferase immunoreactivity in the Macaca fascicularis and Macaca mulatta monkeys. J Comp Neurol 355:135–170.

Bach DR, Weiskopf N, Dolan RJ. 2011. A stable sparse fear memory trace in human amygdala. J Neurosci 31:9383–9389.

Baddeley A. 2007. Working Memory, Thought, and Action. Oxford: Oxford University Press.

Baddeley A, Eysench MW, Anderson MC. 2009. Memory. Hove: Psychology Press.

Bang SJ, Brown TH. 2009. Muscarinic receptors in perirhinal cortex control trace conditioning. J Neurosci 29:4346–4350.

Bangasser DA, Waxler DE, Santollo J, Shors TJ. 2006. Trace conditioning and the hippocampus: The importance of contiguity. J Neurosci 26:8702–8706.

Baxter MG, Murray EA. 2001. Opposite relationship of hippocampal and rhinal cortex to delayed nonmatching-to-sample. Hippocampus 11:61–71.

Beggs JM, Moyer JR, McGann JP, Brown TH. 2000. Prolonged synaptic integration in perirhinal cortical neurons. J Neurophysiol 83:3294–3298.

Blair NT, Kaczmarek JS, Clapham DE. 2009. Intracellular calcium strongly potentiates agonist-activated TRPC5 channels. J Gen Physiol 133:525–546.

Brody CD, Romo R, Kepecs A. 2003. Basic mechanisms for graded persistent activity: Discrete attractors, continuous attractors, and dynamic representations. Curr Opin Neurobiol 13:204–211.

Bucci DJ, Phillips RG, Burwell RD. 2000. Contributions of postrhinal and perirhinal cortex to contextual information processing. Behav Neurosci 114:882–894.

Bucher D, Taylor AL, Marder E. 2006. Central pattern generating neurons simultaneously express fast and slow rhythmic activities in the stomatogastric ganglion. J Neurophysiol 95:3617–3632.

Burwell RD, Amaral DG. 1998a. Cortical afferents of the perirhinal, postrhinal, and entorhinal cortices of the rat. J Comp Neurol 398:179–205.

Burwell RD, Amaral DG. 1998b. Perirhinal and postrhinal cortices of the rat: Interconnectivity and connections with the entorhinal cortex. J Comp Neurol 391:293–321.

Carlsen J, Zaborszky L, Heimer L. 2004. Cholinergic projections from the basal forebrain to the basolateral amygdaloid complex: A combined retrograde fluorescent and immunohistochemical study. J Comp Neurol 234:155–167.

Chowdhury N, Quinn JJ, Fanselow MS. 2005. Dorsal hippocampus involvement in trace fear conditioning with long, but not short, trace intervals in mice. Behav Neurosci 119:1396–1402.

Compte A, Brunel N, Goldman-Rakic PS, Wang XJ. 2000. Synaptic mechanisms and network dynamics underlying spatial working memory in a cortical network model. Cereb Cortex 10:910–923.

Constantinidis C, Wang XJ. 2004. A neural circuit basis for spatial working memory. Neuroscientist 10:553–565.

Czerniawski J, Yoon T, Otto T. 2009. Dissociating space and trace in dorsal and ventral hippocampus. Hippocampus 1:20–32.

Durstewitz D, Seamans JK, Sejnowski TJ. 2000. Neurocomputational models of working memory. Nat Neurosci 3Suppl:1184–1191.

Egorov AV, Hamam BN, Fransen E, Hasselmo ME, Alonso AA. 2002. Graded persistent activity in entorhinal cortex neurons. Nature 420:173–178.

Egorov AV, Unsicker K, von Bohlen und Halbach O. 2006. Muscarinic control of graded persistent activity in lateral amygdala neurons. Eur J Neurosci 24:3183–3194.

Eichenbaum H, Otto T, Cohen NJ. 1994. Two functional components of the hippocampal memory system. Behav Brain Sci 17:449–472.

Esclassan F, Coutureau E, Di Scala G, Marchand AR. 2009. A cholinergic-dependent role for the entorhinal cortex in trace fear conditioning. J Neurosci 29:8087–8093.

Fanselow MS, Poulos AM. 2005. The neuroscience of mammalian associative learning. Annu Rev Psychol 56:207–234

Faulkner B, Brown TH. 1999. Morphology and physiology of neurons in the rat perirhinal-lateral amygdala area. J Comp Neurol 411:613–642.

Fransen E, Tahvildari B, Egorov AV, Hasselmo ME, Alonso AA. 2006. Mechanism of graded persistent cellular activity of entorhinal cortex layer v neurons. Neuron 49:735–746.

Furtak SC, Moyer JR, Brown TH. 2007a. Morphology and ontogeny of rat perirhinal cortical neurons. J Comp Neurol 505:493–510.

Furtak SC, Wei SM, Agster KL, Burwell RD. 2007b. Functional neuroanatomy of the parahippocampal region in the rat: The perirhinal and postrhinal cortices. Hippocampus 17:709–722.

Hasselmo ME. 2006. The role of acetylcholine in learning and memory. Curr Opin Neurobiol 16:710–715.

Hasselmo ME, Stern CE. 2006. Mechanisms underlying working memory for novel information. Trends Cogn Sci 10:487–493.

Helmstetter FJ, Parsons RG, Gafford GM. 2008. Macromolecular synthesis, distributed synaptic plasticity, and fear conditioning. Neurobiol Learn Mem 89:324–337.

Johnston D, Narayanan R. 2008. Active dendrites: Colorful wings of the mysterious butterflies. Trends Neurosci 31:309–316.

Jonides J, Lewis RL, Nee DE, Lustig CA, Berman MG, Moore KS. 2008. The mind and brain of short-term memory. Annu Rev Psychol 59:193–224.

Kent BA, Baysinger AN, Brown TH. Selective control of trace fear conditioning by muscarinic receptors in the amygdala. Soc Neurosci Abstr (in press).

Kerr KM, Agster KL, Furtak SC, Burwell RD. 2007. Functional neuroanatomy of the parahippocampal region: The lateral and medial entorhinal areas. Hippocampus 17:697–708.

Kholodar-Smith DB, Allen TA, Brown TH. 2008a. Fear conditioning to discontinuous auditory cues requires perirhinal cortical function. Behav Neurosci 122:1178–1185.

Kholodar-Smith DB, Boguszewski P, Brown TH. 2008b. Auditory trace fear conditioning requires perirhinal cortex. Neurobiol Learn Mem 90:537–543.

Kim JJ, Jung MW. 2006. Neural circuits and mechanisms involved in Pavlovian fear conditioning: A critical review. Neurosci Biobehav Rev 30:188–202.

Lau PM, Bi GQ. 2005. Synaptic mechanisms of persistent reverberatory activity in neuronal networks. Proc Natl Acad Sci U S A 102:10333–10338.

Lindquist DH, Jarrard LE, Brown TH. 2004. Perirhinal cortex supports delay fear conditioning to rat ultrasonic social signals. J Neurosci 24:3610–3617.

Magee JC, Johnston D. 2005. Plasticity of dendritic function. Curr Opin Neurobiol 15:334–342.

Major G, Tank D. 2004. Persistent neural activity: Prevalence and mechanisms. Curr Opin Neurobiol 14:675–684.

Maren S, Quirk GJ. 2004. Neuronal signaling of fear memory. Nature 5:844–852.

McEchron MD, Bouwmeester H, Tseng W, Weiss C, Disterhoft JF. 1998. Hippocampectomy disrupts auditory trace fear conditioning and contextual fear conditioning in the rat. Hippocampus 8:638–646.

McGann JP, Moyer JR, Brown TH. 2001. Predominance of late-spiking neurons in layer VI of rat perirhinal cortex. J Neurosci 21:4969–4976.

McGaughy J, Koene RA, Eichenbaum H, Hasselmo ME. 2005. Cholinergic deafferentation of the entorhinal cortex in rats impairs encoding of novel but not familiar stimuli in a delayed nonmatch-to-sample task. J Neurosci 25:10273–10281.

Mesulam M. 2004. The cholinergic innervation of the human cerebral cortex. Prog Brain Res 148:67–78.

Misane I, Tovote P, Meyer M, Spiess J, Ogren SO, Stiedl O. 2005. Time dependent involvement of the dorsal hippocampus in trace fear conditioning in mice. Hippocampus 15:418–426.

Mongillo G, Barak O, Tsodyks M. 2008. Synaptic theory of working memory. Science 319:1543–1546.

Moyer JR, Brown TH. 2006. Impaired trace and contextual fear conditioning in aged rats. Behav Neurosci 120:612–624.

Moyer JR, Brown TH. 2007. Visually-guided patch-clamp recordings in brain slices. In: Walz W, editor. Patch-Clamp Analysis: Advanced Techniques,2nd ed. Totowa, NJ: Humana Press. pp169–227.

Moyer JR, Deyo RA, Disterhoft JF. 1990. Hippocampectomy disrupts trace eye-blink conditioning in rabbits. Behav Neurosci 10:243–252.

Moyer JR, McNay E, Brown TH. 2002. Three classes of pyramidal neurons in layer V of rat perirhinal cortex. Hippocampus 12:218–234.

Mozzachiodi R, Byrne JH. 2010. More than synaptic plasticity: Role of nonsynaptic plasticity in learning and memory. Trends Neurosci 33:17–26.

Parsana AJ, Brown TH. 2010. Temporal lobes and object recognition. In: Koob GF, Le Moal M, Thompson RF, editors.Encyclopedia of Behavioral Neuroscience, Vol 3. Oxford: Academic Press. pp375–382.

Pare D, Quirk GJ, LeDoux JE. 2004. New vistas on amygdala networks in conditioned fear. J Neurophysiol 92:1–9.

Phelps EA, LeDoux JE. 2005. Contributions to the lamygdala to emotion processing: From animal models to human behavior. Neuron 48:175–187.

Pikkarainen M, Pitkanen A. 2001. Projections from the lateral, basal and accessory basal nuclei of the amygdala to the perirhinal and postrhinal cortices in rat. Cereb Cortex 11:1064–1082.

Pitkanen A, Pikkarainen M, Nurminen N, Ylinen A. 2000. Reciprocal connections between the amygdala and the hippocampal formation, perirhinal cortex, and postrhinal cortex in rat. Ann N Y Acad Sci 911:369–391.

Quinn JJ, Oommen SS, Morrison GE, Fanselow MS. 2002. Post-training excitotoxic lesions of the dorsal hippocampus attenuate forward trace, backward trace, and delay fear conditioning in a temporally specifc manner. Hippocampus 12:495–504.

Ramsey IS, Delling M, Clapham DE. 2006. An introduction to TRP channels. Annu Rev Physiol 68:619–647.

Raybuck JD, Lattal KM. 2011. Double dissociation of amygdala and hippocampal contributions to trace and delay fear conditioning. PLoS One 6:e15982.

Reboreda A, Raouf R, Alonso A, Seguela P. 2007. Development of cholinergic modulation and graded persistent activity in layer v of medial entorhinal cortex. J Neurophysiol 97:3937–3947.

Reboreda A, Jimenez-Diaz L, Navarro-Lopez JD. 2011. TRP channels and neural persistent plasticity. In: Islam MS, editor.Transient Receptor Potential Channels. Adv Exp Med Biol 704:595–613.

Rodriguez P, Levy WB. 2001. A model of hippocampal activity in trace conditioning: Where's the trace? Behav Neurosci 115:1224–1238.

Seeger T, Fedoroval I, Zheng F, Miyakawa T, Koustova E, Gomeza J, Basile AS, Alzheimer C, Wess J. 2004. M2 muscarinic acetylcholine receptor knock-out mice show deficits in behavioral flexibility, working memory, and hippocampal plasticity. J Neurosci 24:10117–10127.

Solomon PR, Vander Schaaf ER, Thompson RF, Weisz DJ. 1986. Hippocampus and trace conditioning of the rabbit's classically conditioned nictitating membrane response. Behav Neurosci 100:729–744.

Tahvildari B, Fransen E, Alonso AA, Hasselmo ME. 2007. Switching between "On" and "Off" states of persistent activity in lateral entorhinal layer III neurons. Hippocampus 17:257–263.

Teramae JN, Fukai T. 2005. A cellular mechanism for graded persistent activity in a model neuron and its implications in working memory. J Comput Neurosci 18:105–121.

Vaucher E, Hamel E. 1995. Cholinergic basal forebrain neurons project to cortical microvessels in the rat: Electron microscopic study with anterogradely transported Phaseolus vulgaris leucoagglutinin and choline acetyltransferase immunocytochemistry. J Neurosci 15:7427–7441.

Venkatachalam K, Montell C. 2007. TRP channels. Annu Rev Biochem 76:387–417.

Wang D, Grillner S, Wallen P. 2006. Effects of flufenamic acid on fictive locomotion, plateau potentials, calcium channels and NMDA receptors in the lamprey spinal cord. Neuropharmacology 51:1038–1046.

Winters BD, Bussey TJ. 2005. Removal of cholinergic input to perirhinal cortex disrupts object recognition but not spatial working memory in the rat. Eur J Neurosci 21:2263–2270.

Woodruff-Pak DS, Disterhoft JF. 2008. Where is the trace in trace conditioning? Trends Neurosci 31:105–112.

Yan HD, Villalobos C, Andrade R. 2009. TRPC channels mediate a muscarinic receptor-induced afterdepolarization in cerebral cortex. J Neurosci 29:10038–10046.

Yoon T, Otto T. 2007. Differential contributions of dorsal vs. ventral hippocampus to auditory trace fear conditioning. Neurobiol Learn Mem 87:464–475.

Yoshida M, Hasselmo ME. 2009. Persistent firing supported by an intrinsic cellular mechanism in a component of the head direction system. J Neurosci 29:4945–4952.

Yoshida M, Fransen E, Hasselmo ME. 2008. mGluR-dependent persistent firing in entorhinal cortex layer III neurons. Eur J Neurosci 28:1116–1126.

Young BJ, Otto T, Fox GD, Eichenbaum H. 1997. Memory representation within the parahippocampal region. J Neurosci 17:5183–5195.

Zhang Z, Seguela P. 2010. Metabotropic induction of persistent activity in layers II/III of anterior cingulate cortex. Cerebral Cortex 20:2948–2957.

Zhang Z, Reboreda A, Alonso A, Barker PA, Seguela P. 2011. TRPC channels underlie cholinergic plateau potentials and persistent activity in entorhinal cortex. Hippocampus 21:386–97.